



**HAL**  
open science

# Distributed time-varying formation tracking of multi-quadrotor systems with partial aperiodic sampled data

Syed Ali Ajwad, Emmanuel Moulay, Michael Defoort, Tomas Menard, P. Coirault

## ► To cite this version:

Syed Ali Ajwad, Emmanuel Moulay, Michael Defoort, Tomas Menard, P. Coirault. Distributed time-varying formation tracking of multi-quadrotor systems with partial aperiodic sampled data. *Nonlinear Dynamics*, 2022, 108 (3), pp.2263-2278. 10.1007/s11071-022-07294-w . hal-03596635

**HAL Id: hal-03596635**

**<https://hal.science/hal-03596635>**

Submitted on 3 Mar 2022

**HAL** is a multi-disciplinary open access archive for the deposit and dissemination of scientific research documents, whether they are published or not. The documents may come from teaching and research institutions in France or abroad, or from public or private research centers.

L'archive ouverte pluridisciplinaire **HAL**, est destinée au dépôt et à la diffusion de documents scientifiques de niveau recherche, publiés ou non, émanant des établissements d'enseignement et de recherche français ou étrangers, des laboratoires publics ou privés.

1 **Distributed time-varying formation tracking of**  
2 **multi-quadrotor systems with partial aperiodic**  
3 **sampled data**

4 **Syed Ali Ajwad · Emmanuel Moulay ·**  
5 **Michael Defoort · Tomas Ménard ·**  
6 **Patrick Coirault**

7  
8 Received: DD Month YEAR / Accepted: DD Month YEAR

9 **Abstract** In this article, a distributed formation tracking controller is pro-  
10 posed for Multi-Agent Systems (MAS) consisting of quadrotors. It is con-  
11 sidered that each quadrotor in the MAS only shares its translation position  
12 information with its neighbors. Moreover, position information is transmitted  
13 at nonuniform and asynchronous time instants. The control system is divided  
14 into an outer-loop for the position control and an inner-loop for the attitude  
15 control. A continuous-discrete time observer is used in the outer-loop to esti-  
16 mate both position and velocity of the the quadrotor and its neighbors using  
17 discrete position information it receives. Then, these estimated states are used  
18 to design the position controller in order to enable quadrotors to generate the  
19 required geometric shape. A finite-time attitude controller is designed to track  
20 the desired attitude as dictated by the position controller. Finally, a closed-

---

S. A. Ajwad  
LIAS (EA 6315), Université de Poitiers, 2 rue Pierre Brousse, 86073 Poitiers Cedex 9, France  
E-mail: syed.ali.ajwad@univ-poitiers.fr

E. Moulay  
XLIM (UMR CNRS 7252), Université de Poitiers, 11 bd Marie et Pierre Curie, 86073 Poitiers  
Cedex 9, France  
E-mail: emmanuel.moulay@univ-poitiers.fr

M. Defoort  
LAMIH UMR CNRS 8201, INSA Hauts-de-France, Polytechnic University Hauts-de-France,  
59313 Valenciennes, France  
E-mail: michael.defoort@uphf.fr

T. Ménard  
LAC (EA 7478), Normandie Université, UNICAEN, 6 bd du Maréchal Juin, 14032 Caen  
Cedex, France  
E-mail: tomas.menard@unicaen.fr

P. Coirault  
LIAS (EA 6315), Université de Poitiers, 2 rue Pierre Brousse, 86073 Poitiers Cedex 9, France  
E-mail: patrick.coirault@univ-poitiers.fr

loop stability analysis of the overall system including nonlinear coupling is performed.

**Keywords** Multi-agent systems, Quadrotor, Continuous-discrete time observers, Distributed control, Under-actuated system.

## 1 Introduction

In recent years, the study of Unmanned Air Vehicles (UAV) has attracted much attention due to their vast range of applications in defence, agriculture, transportation, disaster management, entertainment etc. (see for instance [1, 2, 3]). Quadrotor UAV is more popular among other UAVs due to its distinctive characteristics like simple structure, fast maneuverability and vertical take off and landing ability [4]. Compared to a single quadrotor operation, the use of multiple quadrotors working in a cooperative manner has some clear advantages such as high efficiency, flexibility, wide coverage area, robustness, etc.

Formation control or formation tracking of cooperative Multi-Agent System (MAS) is considered as one of the fundamental problems in which agents are required to produce a desired geometric shape in order to accomplish some tasks. Multi-quadrotor formation tracking has various applications both in civilian and military domains. These applications include (but are not limited to) target enclosure and tracking, search and rescue, surveillance, heavy payload transportation and telecommunication relay [5, 6, 7]. The problem of formation control and tracking has been extensively studied in the literature [8, 9, 10, 11, 12]. Formation control techniques are usually categorized as virtual structure [13], behavior-based [14] and leader-follower [15]. Distributed consensus based formation control is another interesting approach in which all above mentioned categories can be incorporated [16]. A consensus-based formation tracking algorithm for second-order MAS has been proposed in [17]. In [18], the formation control problem of MAS with switching topology has been discussed for second-order agent dynamics. A fixed-time formation tracking controller has been proposed for MAS using adaptive neural networks and minimal learning parameter based approach [19]. The problem of formation control for high-order nonlinear systems has been studied in [12, 20].

Nevertheless, it should be noted that the extension of formation tracking algorithms designed for first-order, second-order or even high-order nonlinear MAS to multi-quadrotor systems is not trivial. Indeed, the control design for quadrotors is considered as a complex problem because such systems are not only inherently nonlinear but also under-actuated. The control of multiple quadrotors in a distributed manner becomes even more complex. There exist some works in the literature dealing with the problem of formation control for multi-quadrotors. For instance, a consensus based fixed formation tracking controller has been proposed for multi-quadrotor systems in [21]. In this work, it was considered that the quadrotor flies slowly and propeller respond is very high. The nonlinearity of the system was ignored by linearizing its

64 vertical model around the equilibrium point and the horizontal movement  
65 was described as a fourth-order system. A consensus based formation track-  
66 ing controller has been designed in [22] where the quadrotor dynamics was  
67 divided into two subsystems describing horizontal and vertical motion sep-  
68 arately. The formation tracking problem of multi-quadrotor systems in the  
69 presence of switching topology has been discussed in [23] using a hierarchical  
70 controller for each quadrotor based on position and attitude loops. In [24], a  
71 formation tracking algorithm for time-varying formation has been presented. A  
72 formation tracking control scheme has been proposed in [25] where the position  
73 and attitude dynamics are considered as two subsystems and two controllers  
74 are designed separately to control both subsystems. However, the closed-loop  
75 stability analysis was not provided.

76 Another important issue in the above mentioned algorithms is the assump-  
77 tion that both position and velocity states are shared between the neighbours  
78 in continuous time. However, in order to reduce the cost and size of the quadro-  
79 tor, it is of great interest to use a minimum number of sensors. Furthermore,  
80 the network may have limited communication resources. It is always more cost  
81 effective if the neighbors only share partial data as it requires less communica-  
82 tion bandwidth. Therefore, it is not always possible or feasible to transmit the  
83 whole state. Similarly, only discrete data can be shared due to digital nature of  
84 the communication equipment. Furthermore, transmitting data with uniform  
85 and synchronized sampling time is also not possible in many practical appli-  
86 cations. To deal with these above mentioned communication constraints, a  
87 continuous-discrete time observer based algorithm for consensus (resp. forma-  
88 tion tracking) has been proposed [26] (resp. [27, 28]). However, these articles  
89 only focus on double-integrator MAS systems. A leader-following consensus  
90 algorithm for a fully actuated  $N$ -order MAS with Lipschitz nonlinearities is  
91 presented in [29]. However, it is not straightforward to extend this technique  
92 for the time-varying formation tracking problem of under-actuated nonlinear  
93 multi-quadrotor systems.

94 Inspired by the above discussion, in this paper, a distributed time-varying  
95 formation tracking strategy is designed for under-actuated multi-quadrotor  
96 systems with communication constraints. It is considered that each quadrotor  
97 only shares its translation position information with its neighbors. Velocity and  
98 acceleration information is not available. Moreover, the sampling rate at which  
99 the position data is transmitted is nonuniform and asynchronous. As men-  
100 tioned above, irregular and asynchronous sampling is inevitable in all practical  
101 applications and exchange of partial state is always cost effective. Therefore,  
102 our designed algorithm is useful in all practical applications of multi-quadrotor  
103 formation tracking. In the current article, the control system of each quadrotor  
104 in the network is divided into a position subsystem (outer-loop) and an atti-  
105 tude subsystem (inner-loop). Both subsystems are coupled with a nonlinear  
106 coupling term. First, in the outer-loop, a distributed consensus based position  
107 formation tracking algorithm is designed. A continuous-discrete time observer  
108 is used to reconstruct both position and velocity in continuous time using  
109 the available discrete position data. Then, a finite-time control algorithm is

used in the inner-loop to track the desired attitude. Finally, the stability of the closed-loop system, which includes the nonlinear coupling term, is proved. This kind of cascaded controller architecture for a single quadrotor can be found in the literature [30, 31]. However, the closed-loop stability for multi-quadrotor systems with two coupled control loops has never been carefully analyzed. The stability analysis of multi-quadrotor systems is always more complex when compared to single quadrotor systems especially when multi-quadrotor systems are subjects to communication constraints. The proposed strategy yields first results of outer-inner loop based multi-quadrotor formation control in the presence of communication constraints. The efficiency of the proposed algorithm is shown through simulation results.

The remaining of the paper is organized as follows. Section 2 provides some preliminaries on graph theory while Section 3 describes the system modeling and problem statement. Main results are presented in Section 4 which include controller design and stability analysis. Simulation results are given in Section 5 while the paper is concluded in Section 6.

## 2 Preliminaries

The communication topology among the agents in a MAS can be described by a graph. Let  $\mathcal{G} = (\mathcal{V}, \mathcal{E})$  be a  $N$ -order directed graph with  $\mathcal{V} = \{v_1, v_2 \dots v_N\}$  denoting a nonempty and finite set of nodes while  $\mathcal{E} \subseteq \mathcal{V} \times \mathcal{V}$  represents a set of edges.  $(v_i, v_j)$  is an edge of  $\mathcal{G}$  which describes that node  $v_j$  can receive data from node  $v_i$ . In a directed graph,  $(v_i, v_j) \in \mathcal{E}$  does not imply that  $(v_j, v_i) \in \mathcal{E}$ .  $\mathcal{A} = [a_{ij}]_{N \times N}$  is the adjacency matrix with  $a_{ij} = 1$  if  $(v_i, v_j) \in \mathcal{E}$  and  $a_{ij} = 0$  otherwise.  $\mathcal{L} = [l_{ij}]_{N \times N}$  is the Laplacian matrix given as  $l_{ii} = \sum_{j \neq i} a_{ij}$ ,  $l_{ij} = -a_{ij}$  for  $i \neq j$ . The connectivity between the leader and the  $N$  followers is given by a diagonal matrix  $\mathcal{B} = \text{diag}(b_1, b_2, \dots, b_N)$  such that  $b_i = 1$  if follower  $i$  can receive information from the leader and  $b_i = 0$  otherwise. A graph has a directed spanning tree if there exists a directed path from the root to all other nodes. See Appendix B of [32] for further details on graph theory.

**Assumption 1** *It is assumed that there exists at least one directed spanning tree with the leader as a root, i.e there is at least one directed path from the leader to all the followers.*

Matrix  $\mathcal{H} = \mathcal{L} + \mathcal{B}$  is a nonsingular M-matrix due to Assumption 1 [33]. Furthermore, there exists a diagonal matrix  $\Omega = \text{diag}(\omega_1, \dots, \omega_N)$  such that  $\mathcal{H}^T \Omega + \Omega \mathcal{H} > 0$  [34]. Let

$$\omega_{max} = \max\{\omega_1, \dots, \omega_N\} \quad (1)$$

$$\rho = \lambda_{min}(\mathcal{H}^T \Omega + \Omega \mathcal{H}) \quad (2)$$

where  $\lambda_{min}(\cdot)$  represents the corresponding smallest eigenvalue.

### 147 3 Problem statement

#### 148 3.1 System modeling

149 Let us consider a multi-quadrotor system consisting of  $N$  quadrotors. Let the  
 150 position of the  $i$ -th quadrotor in the inertial frame  $\{I\}$  be represented as  
 151  $\xi_i = [x_i \ y_i \ z_i]^T$  while the Euler angles are  $\eta_i = [\phi_i \ \theta_i \ \psi_i]^T$  where  $\phi_i$ ,  $\theta_i$  and  
 152  $\psi_i$  represent roll, pitch and yaw angles respectively in the body frame  $\{B\}$  as  
 153 shown in Figure 1.

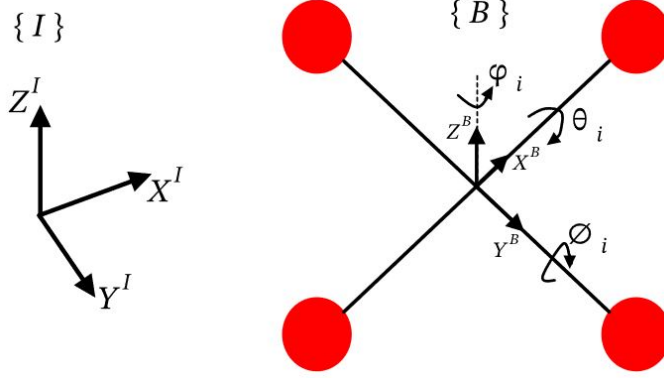


Fig. 1: Inertial and body frames for a quadrotor system.

154 The quadrotor position dynamics is given as

$$\begin{cases} \ddot{x}_i = \frac{T_i}{m_i} (\cos \phi_i \sin \theta_i \cos \psi_i + \sin \phi_i \sin \psi_i), & i = 1, \dots, N \\ \ddot{y}_i = \frac{T_i}{m_i} (\cos \phi_i \sin \theta_i \sin \psi_i - \sin \phi_i \cos \psi_i) \\ \ddot{z}_i = \frac{T_i}{m_i} (\cos \phi_i \cos \theta_i) - g \end{cases} \quad (3)$$

155 where  $T_i$  is the total thrust,  $m_i$  represents the mass of quadrotor  $i$  while  $g$   
 156 denotes the acceleration due to gravity. The attitude dynamics of quadrotor  $i$   
 157 can be represented as

$$\begin{cases} \dot{\eta}_i = W_i \Omega_i \\ I_i \dot{\Omega}_i = \Omega_i^* I_i \Omega_i + \tau_i \end{cases} \quad (4)$$

158 where  $\Omega_i = [\omega_{i,1} \ \omega_{i,2} \ \omega_{i,3}]^T$  represents angular velocities in the body frame  
 159 while  $\Omega_i^*$  is its skew-symmetric matrix

$$\Omega_i^* = \begin{bmatrix} 0 & -\omega_{i,3} & \omega_{i,2} \\ \omega_{i,3} & 0 & -\omega_{i,1} \\ -\omega_{i,2} & \omega_{i,1} & 0 \end{bmatrix} \quad (5)$$

160  $I_i = \text{diag}\{I_{i,1}, I_{i,2}, I_{i,3}\}$  is the inertia matrix in the body frame,  $\tau_i = [\tau_{\phi_i} \ \tau_{\theta_i} \ \tau_{\psi_i}]^T$   
 161 represents the torque vector and  $W_i$  is the orthogonal rotation matrix given  
 162 as

$$W_i = \begin{bmatrix} 1 & \sin \phi_i \tan \theta_i & \cos \phi_i \tan \theta_i \\ 0 & \cos \phi_i & -\sin \phi_i \\ 0 & \frac{\sin \phi_i}{\cos \theta_i} & \frac{\cos \phi_i}{\cos \theta_i} \end{bmatrix} \quad (6)$$

163 The quadrotors dynamics (3) and (4) can be written in a more compact form  
 164 as

$$\begin{cases} \ddot{\xi}_i = \frac{T_i}{m_i} \mathcal{R}_B^T e_3 - g e_3, & i = 1, \dots, N \\ \ddot{\eta}_i = \dot{W}_i \Omega_i + W_i I_i^{-1} \Omega_i^* I_i \Omega_i + W_i I_i^{-1} \tau_i \end{cases} \quad (7)$$

165 where  $e_3 = [0, 0, 1]^T$  while  $\mathcal{R}_B^T \in SO(3)$  denotes the rotation matrix between  
 166 the body frame and the inertial frame

$$\mathcal{R}_B^T = \begin{bmatrix} c\theta_i c\psi_i & s\phi_i s\theta_i c\psi_i - c\phi_i s\psi_i & c\phi_i s\theta_i c\psi_i + s\phi_i s\psi_i \\ c\theta_i s\psi_i & s\phi_i s\theta_i c\psi_i + c\phi_i s\psi_i & c\phi_i s\theta_i c\psi_i - s\phi_i s\psi_i \\ -s\theta_i & s\phi_i c\theta_i & c\phi_i c\theta_i \end{bmatrix} \quad (8)$$

167 where  $c$  and  $s$  represent  $\cos(\cdot)$  and  $\sin(\cdot)$ , respectively.

168 The overall quadrotor system is under-actuated since there are four control  
 169 inputs  $(T_i, \tau_{\phi_i}, \tau_{\theta_i}, \tau_{\psi_i})$  and six outputs  $(x_i, y_i, z_i, \phi_i, \theta_i, \psi_i)$ . Therefore, it is  
 170 not possible to control all the outputs directly. However, if only the attitude  
 171 dynamics is considered, it is clear that it is fully actuated. Hence, (7) can be  
 172 written as

$$\begin{cases} \ddot{\xi}_i = \frac{T_i}{m_i} \mathcal{R}_B^T e_3 - g e_3 \\ \ddot{\eta}_i = \tilde{\tau}_i \end{cases} \quad (9)$$

173 with  $\tilde{\tau}_i = \dot{W}_i \Omega_i + W_i I_i^{-1} \Omega_i^* I_i \Omega_i + W_i I_i^{-1} \tau_i$ .

### 174 3.2 Problem formulation

175 The desired formation pattern can be defined by a formation vector  $F(t) =$   
 176  $[f_1(t)^T \dots f_N(t)^T]$  where  $f_i(t) = [f_{i,\xi}^T, f_{i,v}^T]$  satisfies

$$\dot{f}_{i,\xi} = f_{i,v}$$

177 for  $i = 1, \dots, N$ .  $f_{i,\xi}, f_{i,v} \in \mathbb{R}^3$  are the corresponding position and velocity  
 178 offsets of quadrotor  $i$  with respect to the reference trajectory  $r_0 = [\xi_0 \ \dot{\xi}_0]^T$   
 179 where  $\xi_0 = [x_0 \ y_0 \ z_0]$ . The reference trajectory can be independently produced  
 180 by a real or virtual leader denoted with 0. It is worth noting that the formation  
 181 vector  $f_i$  only describes the offset with respect to the leader and does not  
 182 represent formation coordinates in the global frame. To further explain the

183 notation of formation vector  $f_i(t)$ , let us consider a network of quadrotors  
 184 with a leader and three followers. Let the formation vector be chosen as

$$f_i(t) = \begin{pmatrix} 10 \cos(0.1t + 2\pi(i-1)/3) \\ 10 \sin(0.1t + 2\pi(i-1)/3) \\ 3(i-1) - 3 \\ -\sin(0.1t + 2\pi(i-1)/3) \\ \cos(0.1t + 2\pi(i-1)/3) \\ 0 \end{pmatrix} \quad (10)$$

185 for  $i = 1, 2, 3$ . This formation vector defines that the followers move around the  
 186 leader in a circle of radius 10m with a phase difference of  $2\pi/3$ . The altitude  
 187 position offsets are constant with values  $-3\text{m}$ ,  $0\text{m}$  and  $3\text{m}$  for follower 1, 2 and  
 188 3 respectively. A visual illustration of this formation is provided in Figure 2.

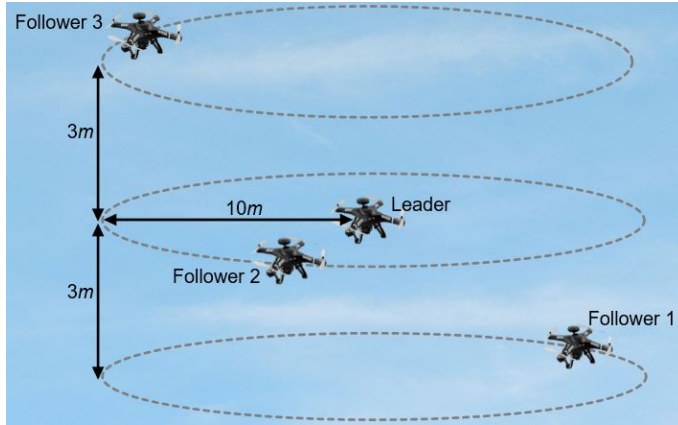


Fig. 2: Example of time-varying formation.

189 **Definition 1** The formation tracking problem of a multi-quadrotor system is  
 190 said to be practically solved if there exists  $\bar{\epsilon} \geq 0$  such that

$$\limsup_{t \rightarrow +\infty} \|r_i(t) - f_i - r_0(t)\| \leq \bar{\epsilon}, \quad i = 1, \dots, N$$

191 where  $r_i = [\xi_i \ \dot{\xi}_i]^T$  for  $i = 1, \dots, N$ .

192 The objective of quadrotors is to achieve time-varying formation in the 3D  
 193 plane. It is considered that each quadrotor in the network sends only its posi-  
 194 tion state to its neighbors at nonuniform and asynchronous sampling times.  
 195 Only a few quadrotors in the network have access to the discrete reference  
 196 position. Let  $t_k^{i,j}$  be the instant when quadrotor  $j$  transmits its position infor-  
 197 mation to quadrotor  $i$  where  $i = 1, \dots, N$ ,  $j = 0, \dots, N$  ( $j \neq i$ ) and  $k \in \mathbb{N}$   
 198 such that

$$0 < t_{k+1}^{i,j} - t_k^{i,j} < \tau_M$$

199 where  $\tau_M$  is the maximum allowable sampling time.

#### 4 Distributed time-varying formation tracking controller

Let us set  $\xi_{di} = f_{i,\xi} + \xi_0$ . Then, the tracking error vector can be defined as

$$e_{\xi_i} = [\xi_i - \xi_{di}, \dot{\xi}_i - \dot{\xi}_{di}]^T \quad (11)$$

Now let  $\eta_{di} = [\phi_{di} \theta_{di} \psi_{di}]^T$  be the desired attitude. The attitude error vector can be given as

$$e_{\eta_i} = [\eta_i - \eta_{di}, \dot{\eta}_i - \dot{\eta}_{di}]^T \quad (12)$$

Therefore, one can obtain the following expressions

$$\begin{cases} \dot{e}_{\xi_i} = Ae_{\xi_i} + B(\ddot{\xi}_i - \ddot{\xi}_{di}) \\ \dot{e}_{\eta_i} = Ae_{\eta_i} + B(\ddot{\eta}_i - \ddot{\eta}_{di}) \end{cases} \quad (13)$$

with  $A = \begin{pmatrix} 0_3 & I_3 \\ 0_3 & 0_3 \end{pmatrix}$ ,  $B = \begin{pmatrix} 0_3 \\ I_3 \end{pmatrix}$ . Dynamics (9) can be seen as a cascaded structure where position and attitude subsystems are coupled through the rotation matrix  $\mathcal{R}_B^T$ . Indeed, let us define the virtual control  $\mu_i = [\mu_{x_i} \mu_{y_i} \mu_{z_i}]^T$  as in [30]

$$\begin{cases} \mu_{x_i} = \frac{T_i}{m_i}(c\phi_{di}s\theta_{di}c\psi_{di} + s\phi_{di}s\psi_{di}) \\ \mu_{y_i} = \frac{T_i}{m_i}(c\phi_{di}s\theta_{di}s\psi_{di} - s\phi_{di}c\psi_{di}) \\ \mu_{z_i} = \frac{T_i}{m_i}(c\phi_{di}c\theta_{di}) - g \end{cases} \quad (14)$$

The thrust and desired angles can be obtained as

$$T_i = m_i \sqrt{\mu_{x_i}^2 + \mu_{y_i}^2 + (\mu_{z_i} + g)^2} \quad (15)$$

$$\phi_{di} = \sin^{-1} \left( \frac{m_i}{T_i} (\mu_{x_i} \sin \psi_{di} - \mu_{y_i} \cos \psi_{di}) \right) \quad (16)$$

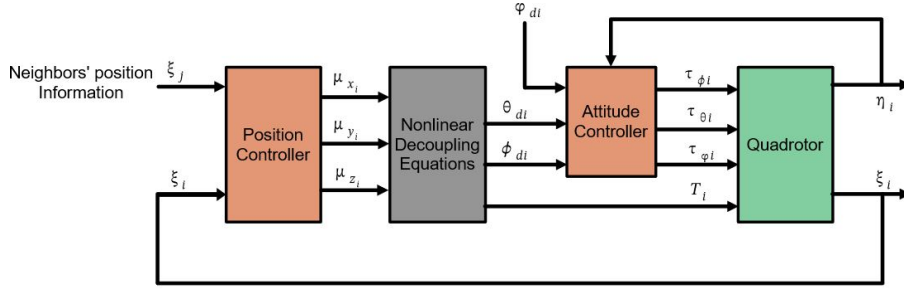
$$\theta_{di} = \tan^{-1} \left( \frac{\mu_{x_i} \cos \psi_{di} + \mu_{y_i} \sin \psi_{di}}{\mu_{z_i} + g} \right) \quad (17)$$

while the desired yaw angle  $\psi_{di}$  is independent of other states. Now introducing  $\mu_i$  and replacing (9) in (13), one can get

$$\begin{cases} \dot{e}_{\xi_i} = \underbrace{Ae_{\xi_i} + B(\mu_i - \ddot{\xi}_{di})}_{f_{\xi_i}} + \underbrace{\frac{T_i}{m_i}BH_i(\eta_i, \eta_{di})}_{f_{\Delta_i}} \\ \dot{e}_{\eta_i} = \underbrace{Ae_{\eta_i} + B(\tilde{\tau}_i - \ddot{\eta}_{di})}_{f_{\eta_i}} \end{cases} \quad (18)$$

where  $H_i(\eta_i, \eta_{di}) = [h_1 \ h_2 \ h_3]^T$  and

$$\begin{cases} h_1 = c\phi_i s\theta_i c\psi_i + s\phi_i s\psi_i - (c\phi_{di} s\theta_{di} c\psi_{di} + s\phi_{di} s\psi_{di}) \\ h_2 = c\phi_i s\theta_i s\psi_i - s\phi_i c\psi_i - (c\phi_{di} s\theta_{di} s\psi_{di} - s\phi_{di} c\psi_{di}) \\ h_3 = c\phi_i c\theta_i - c\phi_{di} c\theta_{di} \end{cases} \quad (19)$$

Fig. 3: Overall control architecture of quadrotor  $i$ 

213 System (18) can be seen as two linear subsystems coupled by a nonlinear term  
 214  $f_{\Delta i}$ . The control objective then becomes to design  $\mu_i$  and  $\tilde{\tau}_i$  such that the  
 215 position and attitude errors converge asymptotically.

216 The overall control design of quadrotor  $i$  can be obtained in the following  
 217 steps:

- 218 1. Design a distributed control scheme  $\mu_i$  for the subsystem  $\dot{e}_{\xi_i} = f_{\xi_i}$  while  
 219 first ignoring the coupling term  $f_{\Delta i}$ ;
- 220 2. Design a control law  $\tilde{\tau}$  for the subsystem  $\dot{e}_{\eta_i} = f_{\eta_i}$  such that the tracking  
 221 error  $e_{\eta_i}$  converges to zero asymptotically;
- 222 3. Finally, consider the closed-loop system including the coupling term  $f_{\Delta i}$   
 223 and show that  $e_{\xi_i}$  and  $e_{\eta_i}$  still converge to zero.

224 Figure 3 shows the control architecture of the  $i^{th}$  quadrotor in the network.

## 225 4.1 Controller Design

### 226 4.1.1 Position controller design

227 Let us first consider the position subsystem. It can be seen that the subsystem  
 228  $\dot{e}_{\xi_i} = f_{\xi_i}$  corresponds to the following dynamics

$$\ddot{\xi}_i = \mu_i \quad (20)$$

229 It is considered that each quadrotor can measure and transmit its position  
 230 state  $\xi_i$  only. The velocity  $\dot{\xi}_i$  and the acceleration  $\ddot{\xi}_i$  are not available. The  
 231 position  $\xi_i$  is transmitted only at irregular and nonuniform time instants. The  
 232 state-space representation of (20) can be given as

$$\begin{cases} \dot{r}_i = Ar_i + B\mu_i \\ y_i = Cr_i \end{cases} \quad (21)$$

233 with  $C = [I_3 \ 0_3]$ . Let us consider that the reference trajectory is produced by  
 234 a virtual leader with the same dynamics, i.e.,

$$\begin{cases} \dot{r}_0 = Ar_0 + B\mu_0 \\ y_0 = Cr_0 \end{cases} \quad (22)$$

235 The input of the leader, i.e.  $\mu_0$ , is not affected by other quadrotors in the  
 236 network. It can be designed to achieve any required reference trajectory for  
 237 the following quadrotors. Only the following assumption is made.

238 **Assumption 2** *The input of the leader  $\mu_0(t)$  is bounded by a constant  $\delta_0 \geq 0$ ,*  
 239 *i.e. one has  $\|\mu_0(t)\| \leq \delta_0$  for all  $t \geq 0$ .*

240 The control input for formation tracking is given by

$$\begin{aligned} \mu_i(t) = & \dot{f}_{i,v} - \bar{c}K_1^2 \left[ \sum_{j=1}^N a_{ij} \left( \hat{\xi}_{i,i}(t) - f_{i,\xi} - \hat{\xi}_{i,j}(t) + f_{j,\xi} \right) \right. \\ & \left. + b_i \left( \hat{\xi}_{i,i}(t) - f_{i,\xi} - \hat{\xi}_{i,0}(t) \right) \right] \\ & - \bar{2c}K_1 \left[ \sum_{j=1}^N a_{ij} \left( \hat{v}_{i,i}(t) - f_{i,v} - \hat{v}_{i,j}(t) + f_{j,v} \right) \right. \\ & \left. + b_i \left( \hat{v}_{i,i}(t) - f_{i,v} - \hat{v}_{i,0}(t) \right) \right] \end{aligned} \quad (23)$$

241 where  $K_1$  and  $\bar{c}$  denote the controller gain and coupling strength respectively  
 242 while  $\hat{\xi}_{i,j} \in \mathbb{R}^3$  and  $\hat{v}_{i,j} \in \mathbb{R}^3$  are the estimated position and velocity of  
 243 quadrotor  $j$  by quadrotor  $i$  and are given by

$$\dot{\hat{r}}_{i,j}(t) = A\hat{r}_{i,j}(t) - K_2\Delta^{-1}K_o e^{-2K_2(t-\kappa_{i,j}(t))} \left( \hat{\xi}_{i,j}(\kappa_{i,j}(t)) - \xi_j(\kappa_{i,j}(t)) \right) \quad (24)$$

244 with  $\hat{r}_{i,j}(t) = \begin{bmatrix} \hat{\xi}_{i,j}^T \\ \hat{v}_{i,j}^T \end{bmatrix}^T$ ,  $\Delta = \begin{pmatrix} I_m & 0_m \\ 0_m & \frac{1}{K_2}I_m \end{pmatrix}$ ,  $K_o = [2I_m \ I_m]^T$  while  $K_2$  rep-  
 245 resents the observer tuning parameter.  $\kappa_{i,j}(t) = \max \left\{ t_k^{i,j} \mid t_k^{i,j} \leq t, k \in \mathbb{N} \right\}$  is  
 246 the last instant when quadrotor  $i$  receives the position data of quadrotor  $j$ . The  
 247 above expression (24) represents a high-gain continuous-discrete time observer  
 248 which estimates position and velocity of a quadrotor as well as its neighbors  
 249 in continuous time from discrete position data.

250 *Remark 1* Here, the coupling strength  $\bar{c}$  is chosen beforehand and remains  
 251 constant for all  $t \geq 0$  since only fixed topology is considered. Therefore, for  
 252 all  $t \geq 0$ , quadrotors only use local information to achieve the required forma-  
 253 tion pattern. The requirement of knowing the communication topology for the  
 254 controller parameters is a common practice in cooperative control. In future  
 255 work, one may investigate the use of adaptive gains to avoid such assumption.

256 *4.1.2 Attitude controller design*

257 First, the following notations are introduced. For any non-negative real number  
258  $\alpha$  and for any  $x \in \mathbb{R}$ ,

$$\text{sig}^\alpha(x) = \text{sign}(x)|x|^\alpha \quad (25)$$

$$\text{fsig}^\alpha(x) = \begin{cases} x, & |x| > 1 \\ \text{sig}^\alpha(x), & |x| \leq 1 \end{cases} \quad (26)$$

259 Let us now consider the attitude subsystem

$$\dot{e}_{\eta_i} = f_{\eta_i} = A e_{\eta_i} + B (\tilde{\tau}_i - \ddot{\eta}_{di}) \quad (27)$$

260 with the following attitude input

$$\tilde{\tau}_i = \ddot{\eta}_{di} - K_3 \text{fsig}^{\alpha_3}(\eta_i - \eta_{di}) - K_4 \text{fsig}^{\alpha_4}(\dot{\eta}_i - \dot{\eta}_{di}) \quad (28)$$

261 where  $K_3, K_4 > 0$ .

262 **Lemma 1** [25] *For the attitude error dynamics (27) with control law (28),*  
263 *the desired attitude is achieved in finite time, i.e.  $\|\eta_i - \eta_{di}\| \rightarrow 0$  if  $\alpha_3$  and  $\alpha_4$*   
264 *are chosen as  $0 < \alpha_3 < 1$  and  $\alpha_4 = 2\alpha_3/(1 + \alpha_3)$ .*

265 *4.2 Closed-loop stability analysis*

266 The following is an important lemma for stability analysis of cascade systems.

267 **Lemma 2** *Let  $v_1(t)$  and  $v_2(t)$  be real valued functions verifying*

$$\begin{aligned} \frac{d}{dt} (v_1^2(t) + v_2^2(t)) &\leq -av_1^2(t) - bv_2^2(t) + c \int_{t-\delta}^t v_2^2(s) ds \\ &\quad + g(t)(v_1^2(t) + v_2^2(t)) + k, \end{aligned} \quad (29)$$

268 *for all  $t \geq 0$ ,  $a, b, c, \delta > 0$ ,  $k \geq 0$  and  $g(t)$  is a decaying function such that for*  
269 *some  $t^* \geq 0$   $g(t) \geq 0$  if  $0 \leq t \leq t^*$  and  $g(t) = 0$  if  $t > t^*$ . There exist  $\gamma \geq 1$ ,*  
270  *$\varrho > 0$ , independent of  $a, b, c, k$ , and  $\bar{\alpha} \geq 0$  such that if  $\delta < \varrho \min(\frac{b}{c}, \frac{1}{\sigma})$ , then*  
271  *$v_1(t)$  and  $v_2(t)$  verify the following inequality*

$$v_1^2(t) + v_2^2(t) \leq \bar{\alpha} e^{-\sigma t} + \frac{\gamma k}{\sigma}, \quad \forall t \geq 0 \quad (30)$$

272 *where  $\sigma$  is given by*

$$\sigma = \frac{1}{2} \min(a, b) \quad (31)$$

273 The proof of Lemma 2 is provided in Appendix A.

274 *Remark 2* It is worth mentioning that Lemma 2 is more general than Lemma  
 275 2 from [29] due to the presence of term  $g(t)(v_1^2(t) + v_2^2(t))$  in (29). Such term  
 276 should be here considered due to the coupling between position subsystem  
 277 (outer-loop) and attitude subsystem (inner-loop), making the stability analysis  
 278 of the closed-loop system in the current paper different from [29].

279 **Theorem 1** *Given the position controller (23) and the attitude controller*  
 280 *(28), if Assumptions 1-2 hold and if the control parameters satisfy*

$$K_2 \leq \frac{\bar{\varrho}}{\tau_M} \quad (32)$$

$$\bar{c} \geq \frac{\omega_{max}}{\rho} \quad (33)$$

$$K_1 = \epsilon K_2 \quad (34)$$

281 *with  $\epsilon \in (0, 1)$  and  $\bar{\varrho} > 0$ , then the formation tracking of the multi-quadrotor*  
 282 *system (9) is achieved in the sense of Definition 1.*

283 *Proof* It is clear from Lemma 1 that the attitude error dynamics  $\dot{e}_{\eta_i} = Ae_{\eta_i} +$   
 284  $B(\tilde{\tau}_i - \ddot{\eta}_{di})$  (given in (18)) using attitude control input (28), converges to zero  
 285 in finite time. Now, it is needed to show that the position error dynamics  
 286 including the coupling term also converges. It is worth mentioning that this  
 287 coupling makes the stability analysis of the closed-loop system in the current  
 288 paper different from [29].

289 The remaining of the proof is divided into several steps. In the first step,  
 290 the dynamics of the position and estimation errors are derived and written  
 291 in a compact form along with the time-varying formation controller (23). App-  
 292 propriate coordinate transformation is also introduced in step 1. Position and  
 293 observer errors are combined in new variables in step 2 to get a more compact  
 294 form. In step 3, candidate Lyapunov functions are introduced and inequalities  
 295 involving their derivatives are derived. Lemma 2 is applied in step 4 to show  
 296 the convergence of the formation tracking error with formation controller (23)  
 297 and (28).

298 *Step 1.* Consider the position error dynamics with the coupling term from (18)

$$\dot{e}_{\xi_i} = \underbrace{Ae_{\xi_i} + B\mu_i - B\mu_0}_{f_{\xi_i}} + \underbrace{\frac{T_i}{m_i}BH_i(\eta_i, \eta_{di})}_{f_{\Delta i}} \quad (35)$$

299 Define the estimation error as  $\tilde{x}_{i,j} = \hat{r}_{i,j} - r_i$  for  $i = 1, \dots, N$  and  $j = 0, \dots, N$ ,  
 300 one has

$$\dot{\tilde{x}}_{i,j}(t) = (A - \theta\Delta^{-1}K_oC)\tilde{x}_{i,j}(t) - \theta\Delta^{-1}K_o z_{i,j}(t) - B\mu_j(t)$$

301 where  $z_{i,j}(t) = [e^{-2\theta(t-\kappa_{i,j}(t))}C\tilde{x}_{i,j}(\kappa_{i,j}(t)) - C\tilde{x}_{i,j}(t)]$ .

302 The position control input can be written as

$$\mu_i = -\bar{c}K_c\Gamma \sum_{k=1}^N \mathcal{H}_{ik}e_{\xi_k} - \bar{c}K_c\Gamma \sum_{k=1}^N \mathcal{H}_{ik}\tilde{x}_{i,k} + b_i\bar{c}K_c\Gamma\tilde{x}_{i,0}$$

303 for  $i = 1, \dots, N$  and  $K_c = B^T Q = (I_3 \ 2I_3)$  with  $Q$  the symmetric positive  
 304 definite matrix solution of  $Q + QA + A^T Q = QB B^T Q$  and  $\Gamma = \begin{pmatrix} K_1^2 I_3 & 0_3 \\ 0_3 & K_1 I_3 \end{pmatrix}$   
 305 Applying the coordinate transformation for high-gain design as  $\bar{e}_{\xi_i} = \Gamma e_{\xi_i}$   
 306 and  $\bar{x}_{i,j} = \Delta \tilde{x}_{i,j}$ , one has

$$\begin{aligned} \dot{\bar{e}}_{\xi_i}(t) &= K_1 A \bar{e}_{\xi_i}(t) + K_1 B \mu_i(t) - K_1 B \mu_0(t) + \frac{K_1 T_i}{m_i} B H_i \\ \dot{\bar{x}}_{i,j}(t) &= K_2 (A - K_o C) \bar{x}_{i,j}(t) - K_2 K_o z_{i,j}(t) - \frac{1}{K_2} B \mu_j(t) \end{aligned}$$

$$\mu_i = -\bar{c} K_c \sum_{k=1}^N \mathcal{H}_{ik} \bar{e}_{\xi_k} - \bar{c} K_c \Gamma \Delta^{-1} \sum_{k=1}^N \mathcal{H}_{ik} \bar{x}_{i,k} + b_i \bar{c} K_c \Gamma \Delta^{-1} \bar{x}_{i,0}$$

307 *Step 2.* Let  $e_{\xi}^c = [\bar{e}_{\xi_1}^T \dots \bar{e}_{\xi_N}^T]^T$ ,  $\bar{x}_i^o = [(\bar{x}_{i,1})^T \dots (\bar{x}_{i,N})^T]^T$ ,  $i = 1 \dots N$  and  
 308  $\bar{x}_0^o = [(\bar{x}_{1,0})^T \dots (\bar{x}_{N,0})^T]^T$ . The tracking error dynamics can be written in a  
 309 more compact form as

$$\begin{aligned} \dot{e}_{\xi}^c &= K_1 [I_N \otimes A] e_{\xi}^c - \bar{c} K_1 [\mathcal{H} \otimes (BK_c)] e_{\xi}^c - \bar{c} K_1 \sum_{i=1}^N [(\mathcal{D}_i^N \mathcal{H}) \otimes (BK_c \Gamma \Delta^{-1})] \bar{x}_i^o \\ &\quad + \bar{c} K_1 [I_N \otimes (BK_c \Gamma \Delta^{-1})] [\mathcal{B} \otimes I_6] \bar{x}_0^o - K_1 [\mathbf{1}_N \otimes B] \mu_0 + K_1 [I_N \otimes B] F_{\Delta} \end{aligned}$$

310 where  $F_{\Delta} = [\frac{T_1}{m_1} H_1, \dots, \frac{T_N}{m_N} H_N]^T$ .

311 *Step 3.* Now, let us define the following Lyapunov functions

$$\bar{V}_c(e_{\xi}) = e_{\xi}^T [\Omega \otimes Q] e_{\xi} \quad (36)$$

$$V_o(\bar{x}_{i,j}) = (\bar{x}_{i,j})^T P(\bar{x}_{i,j}) \quad (37)$$

$$\bar{V}_o(\bar{x}^o) = \sum_{i=1}^N \sum_{j=0}^N s_{ij} V_o(\bar{x}_{i,j}) \quad (38)$$

312  $s_{ij} = 1$  if quadrotor  $i$  receives information from quadrotor  $j$  and 0 otherwise  
 313 for  $i = 1, \dots, N$ ,  $j = 0, \dots, N$  and  $\bar{x}^o$  is the vector containing all the  $\bar{x}_{i,j}$  such  
 314 that  $s_{ij} = 1$ .

315 The derivative of  $V(e_{\xi})$  can be computed as

$$\begin{aligned} \dot{\bar{V}}_c(e_{\xi}^c) &= K_1 (e_{\xi}^c)^T [\Omega \otimes (A^T Q + QA)] e_{\xi}^c - \bar{c} K_1 (e_{\xi}^c)^T [(\mathcal{H}^T \Omega) \otimes ((BK_c)^T Q)] e_{\xi}^c \\ &\quad - \bar{c} K_1 (e_{\xi}^c)^T [(\Omega \mathcal{H}) \otimes (QBK_c)] e_{\xi}^c + 2\bar{c} K_1 (e_{\xi}^c)^T [\Omega \otimes (QBK_c \Gamma \Delta^{-1})] [\mathcal{B} \otimes I_{2m}] \bar{x}_0^o \\ &\quad - 2\bar{c} K_1 \sum_{i=1}^N (e_{\xi}^c)^T [(\Omega \mathcal{D}_i^N \mathcal{H}) \otimes (QBK_c \Gamma \Delta^{-1})] \bar{x}_i^o \\ &\quad - 2K_1 (e_{\xi}^c)^T [(\Omega \mathbf{1}_N) \otimes (QB)] \mu_0 + 2K_1 (e_{\xi}^c)^T [(\Omega \otimes (QB))] F_{\Delta} \end{aligned}$$

316 One can show that

$$\begin{aligned} &2K_1 (e_{\xi}^c)^T [(\Omega \otimes (QB))] F_{\Delta} \\ &\leq 2K_1 \bar{k}_3 \sqrt{V_c} \sum_{i=1}^N \chi \|e_{\eta_i}\| \left[ \sqrt{V_c(e_{\xi}^c)} + \sum_{k=0}^N s_{i,k} \sqrt{V_o(\bar{x}_{i,k})} \right] \quad (39) \end{aligned}$$

317 where  $\bar{k}_3 = \sqrt{\omega_{\max} \lambda_{\max}(Q)}$ . The derivation of (39) is given in Appendix B.

318 Similarly, one has

$$\begin{aligned} & 2\bar{c}K_1(e_\xi^c)^T[\Omega \otimes (QBK_c\Gamma\Delta^{-1})][\mathcal{B} \otimes I_{2m}]\bar{x}_0^o \\ & - 2\bar{c}K_1 \sum_{i=1}^N (e_\xi^c)^T [(\Omega\mathcal{D}_i^N\mathcal{H}) \otimes (QBK_c\Gamma\Delta^{-1})]\bar{x}_i^o \\ & \leq 2k_1K_1\|\Gamma\Delta^{-1}\|\sqrt{\bar{V}_c(e_\xi)}\sqrt{\bar{V}_o(\bar{x}^o)} \end{aligned} \quad (40)$$

$$-2K_1(e_\xi)^T[(\Omega\mathbf{1}_N) \otimes (QB)]\mu_0 \leq 2K_1\bar{k}_2\delta_0\sqrt{V_c(e_\xi^c)}. \quad (41)$$

319 with  $k_1, \bar{k}_2 \geq 0$  where  $k_1$  and  $k_2$  are independent of the tuning parameters.  
320 and if  $\bar{c} \geq \omega_{\max}/\rho$ , then one has

$$\begin{aligned} & K_1(e_\xi)^T[\Omega \otimes (AQ^T + QA)]e_\xi - \bar{c}K_1(e_{\xi_i})^T[(\mathcal{H}^T\Omega) \otimes ((BK_c)^TQ)]e_\xi \\ & - \bar{c}K_1(e_{\xi_i})^T[(\Omega\mathcal{H}) \otimes (QBK_c)]e_\xi \leq -K_1\bar{V}_c(e_\xi) \end{aligned} \quad (42)$$

321 These inequalities lead to

$$\begin{aligned} \dot{\bar{V}}_c(e_\xi^c) & \leq -K_1\bar{V}_c(e_\xi^c) + 2k_1K_1\|\Gamma\Delta^{-1}\|\sqrt{\bar{V}_c(e_\xi)}\sqrt{\bar{V}_o(\bar{x}^o)} + 2\bar{k}_2K_1\delta_0\sqrt{\bar{V}_c(e_\xi)} \\ & + 2\bar{k}_3K_1\sqrt{\bar{V}_c(e_\xi^c)} \sum_{i=1}^N \chi\|e_{\eta_i}\| \left[ \sqrt{V_c(e_\xi)} + \sum_{k=0}^N s_{i,k}\sqrt{V_o(\bar{x}_{i,k})} \right] \end{aligned}$$

322 Similarly,

$$\begin{aligned} \dot{\bar{V}}_o(\bar{x}^o) & \leq -K_2\bar{V}_o(\bar{x}^o) + 2K_2^2k_4\sqrt{\bar{V}_o(\bar{x}^o)} \int_{t-\tau_M}^t \sqrt{\bar{V}_o(\bar{x}^o(s))} ds \\ & + 2K_1k_6\bar{V}_o(\bar{x}^o) + 2\frac{k_5}{K_2}\sqrt{\bar{V}_o(\bar{x}^o)}\sqrt{\bar{V}_c(e_\xi)} + 2\frac{k_7}{K_2}\delta_0\sqrt{\bar{V}_o(\bar{x}^o)} \end{aligned} \quad (43)$$

323 with  $k_4, k_5, k_6, k_7 \geq 0$  are independent of the tuning parameters.

324 *Step 4.* One has

$$\begin{aligned}
& \frac{d}{dt} \left( \sqrt{\bar{V}_c(e_\xi^c)} + \epsilon^{\frac{3}{2}} K_2^2 \sqrt{\bar{V}_o(\bar{x}^o)} \right) \\
& \leq -\frac{\epsilon K_2}{4} \left( 1 - 4k_5 \epsilon^{\frac{1}{2}} \right) \sqrt{\bar{V}_c(e_\xi^c)} - \frac{\epsilon^{\frac{3}{2}} K_2^3}{4} \left( 1 - 4k_1 \epsilon^{\frac{1}{2}} - 4k_6 \epsilon \right) \sqrt{\bar{V}_o(\bar{x}^o)} \\
& \quad - \frac{\epsilon K_2}{4} \sqrt{\bar{V}_c(e_\xi^c)} - \frac{\epsilon^{\frac{3}{2}} K_2^3}{4} \sqrt{\bar{V}_o(\bar{x}^o)} + k_4 \epsilon^{\frac{3}{2}} K_2^4 \int_{t-\tau_M}^t \sqrt{\bar{V}_o(\bar{x}^o(s))} ds \\
& \quad + \bar{k}_3 \epsilon K_2 \sum_{i=1}^N \chi \|e_{\eta_i}\| \left[ \sqrt{V_c(e_\xi)} + \sum_{k=0}^N s_{i,k} \sqrt{V_o(\bar{x}_{i,k})} \right] + \bar{k}_2 \epsilon K_2 \delta_0 + k_7 \epsilon^{\frac{3}{2}} K_2 \delta_0 \\
& \leq -\frac{\epsilon K_2}{4} \left( 1 - 4k_5 \epsilon^{\frac{1}{2}} \right) \sqrt{\bar{V}_c(e_\xi^c)} - \frac{\epsilon^{\frac{3}{2}} K_2^3}{4} \left( 1 - 4k_1 \epsilon^{\frac{1}{2}} - 4k_6 \epsilon \right) \sqrt{\bar{V}_o(\bar{x}^o)} \\
& \quad - \frac{\epsilon K_2}{4} \sqrt{\bar{V}_c(e_\xi^c)} - \frac{\epsilon^{\frac{3}{2}} K_2^3}{4} \sqrt{\bar{V}_o(\bar{x}^o)} + k_4 \epsilon^{\frac{3}{2}} K_2^4 \int_{t-\tau_M}^t \sqrt{\bar{V}_o(\bar{x}^o(s))} ds \\
& \quad + k_3 \epsilon K_2 \sum_{i=1}^N \chi \|e_{\eta_i}\| \left[ \sqrt{V_c(e_\xi)} + \sqrt{V_o(\bar{x}^o)} \right] + \bar{k}_2 \epsilon K_2 \delta_0 + k_7 \epsilon^{\frac{3}{2}} K_2 \delta_0
\end{aligned}$$

325 with  $k_3 = \bar{k}_3 \sqrt{N} \sqrt{N+1}$ .

326 Selecting  $\epsilon < \epsilon^*$  where  $\epsilon^* = \min \left\{ 1, \frac{1}{(4k_4)^2}, \frac{1}{(8k_1)^2}, \frac{1}{8k_5} \right\}$ , one can achieve

$$\begin{aligned}
& \frac{d}{dt} \left( \sqrt{\bar{V}_c(e_\xi^c)} + \epsilon^{\frac{3}{2}} K_2^2 \sqrt{\bar{V}_o(\bar{x}^o)} \right) \\
& \leq -\frac{\epsilon K_2}{4} \sqrt{\bar{V}_c(e_\xi^c)} - \frac{\epsilon^{\frac{3}{2}} K_2^3}{4} \sqrt{\bar{V}_o(\bar{x}^o)} + k_4 \epsilon^{\frac{3}{2}} K_2^4 \int_{t-\tau_M}^t \sqrt{\bar{V}_o(\bar{x}^o(s))} ds \\
& \quad + k_3 \epsilon K_2 \sum_{i=1}^N \chi \|e_{\eta_i}\| \left[ \sqrt{V_c(e_\xi)} + \sqrt{V_o(\bar{x}^o)} \right] + k_2 \epsilon K_2 \delta \tag{44}
\end{aligned}$$

327 with  $k_2 = \max\{\bar{k}_2, k_7\}$ . From Lemma 1, one knows that the attitude error  
328  $e_{\eta_i} \rightarrow 0$  in finite time which implies that after some time  $t > t_a \geq 0$ ,  $\chi \|e_{\eta_i}\| =$   
329  $0$ .

330 Applying Lemma 2 on (44) with  $a = \frac{\epsilon K_2}{4}$ ,  $b = \frac{\epsilon^{\frac{3}{2}} K_2^3}{4}$ ,  $c = k_4 \epsilon^{\frac{3}{2}} K_2^4$ ,  $g(t) =$   
331  $k_3 \epsilon K_2 \sum_{i=1}^N \chi \|e_{\eta_i}\|$  and  $k = k_2 \epsilon K_2 \delta$ , one has  $\bar{\alpha} > 0$ ,  $\varrho > 0$  and  $\gamma \geq 1$  such  
332 that for

$$\tau_M < \frac{\bar{\varrho}}{K_2}$$

333 with  $\bar{\varrho} = \frac{\varrho}{4k_4}$ , the following inequality is achieved

$$\sqrt{\bar{V}_c(e_\xi^c)} + \epsilon^{\frac{3}{2}} K_2^2 \sqrt{\bar{V}_o(\bar{x}^o)} \leq \bar{\alpha} e^{-\frac{K_1}{8} t} + 8\gamma k_2 \delta_0$$

334 Over-evaluation of the above inequality gives

$$\begin{aligned} \sqrt{\bar{V}_c(e_\xi^c)} &\leq \bar{\alpha}e^{-\frac{K_1}{8}t} + 8\gamma k_2 \delta_0 \\ K_1 k_8 \sum_{i=1}^N \|e_{\xi_i}^c\| &\leq \bar{\alpha}e^{-\frac{K_1}{8}t} + 8\gamma k_2 \delta_0 \end{aligned}$$

335 with  $k_8 = \frac{\sqrt{\lambda_{\min} Q} \sqrt{\omega_{\min}}}{\sqrt{N}}$ . Hence

$$\sum_{i=1}^N \|e_{\xi_i}\| \leq \alpha e^{-\frac{K_1}{8}t} + \frac{\beta \delta_0}{K_1} \quad (45)$$

336 where  $\alpha = \frac{\bar{\alpha}}{K_1 k_8}$  and  $\beta = \frac{8k_2 \gamma}{k_8}$ .

337 *Remark 3* The structure of the proposed observer-based formation tracking  
338 controller has some advantages in the presence of communication delays and  
339 packet loss during communications. Since, for each agent, the corresponding  
340 controller only uses the estimated states provided by the continuous-discrete  
341 observers, the time-varying formation tracking is achieved even in the pres-  
342 ence of communication delays if measured position data is accurately time  
343 stamped. Indeed, in this case, the estimation can be provided as soon as the  
344 data is received. Similarly, in case of packet loss, the observer still provides  
345 the estimation if the next packet is received before the maximum sample time  
346  $\tau_M$ .

347 *Remark 4* Inequality (45) shows that the formation tracking error decays ex-  
348 ponentially and enters in a ball centered at the origin and will remain there  
349 for all future time. This means that practical formation tracking is achieved.  
350 One can observe that the radius of the ball is directly proportional to the up-  
351 per bound of the reference/leader acceleration, i.e.  $\delta_0$ . This implies that if the  
352 leader has a constant velocity then the multi-quadrotor system will achieve  
353 exponential stability. The final error can also be reduced by increasing the  
354 position controller gain  $K_1$ . However,  $K_1$  should always remain less than the  
355 observer gain  $K_2$  to keep the controller dynamics slower than the observer  
356 dynamics.

## 357 5 Simulation results

358 Let us consider a multi-quadrotor system with three followers denoted from 1  
359 to 3 and a leader denoted as 0. The communication topology among them is  
360 shown in Figure 4. It is considered that all the quadrotors in the system have  
361 the same structure and modelling parameters. The mass of each quadrotor con-  
362 sidered is  $m_i = 0.4$  while the inertia matrix is  $I_i = \text{diag}\{0.0025, 0.0026, 0.0028\}$ .  
363 The sampling rate at which the position information is transmitted among the

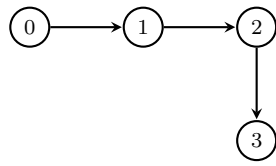


Fig. 4: Communication topology

364 quadrotors is between  $10ms$  and  $100ms$ . The tuning gains for position controller are chosen as  $K_1 = 0.6$ ,  $K_2 = 10$  and  $\bar{c} = 1$ . The tuning parameters of the attitude controller are selected as  $\alpha_3 = \frac{3}{4}$ ,  $\alpha_4 = \frac{6}{7}$ ,  $K_3 = 20$  and  $K_4 = 10$ .

367 The desired time-varying formation vector is selected for  $i = 1, \dots, 3$  as  
 368 given in (10). In the first scenario, the leader is hovering at the altitude of  
 369 10m while the followers start from their initial position and make the required  
 370 formation. Figure 5 shows the formation tracking results while the tracking error is shown in Figure 6.

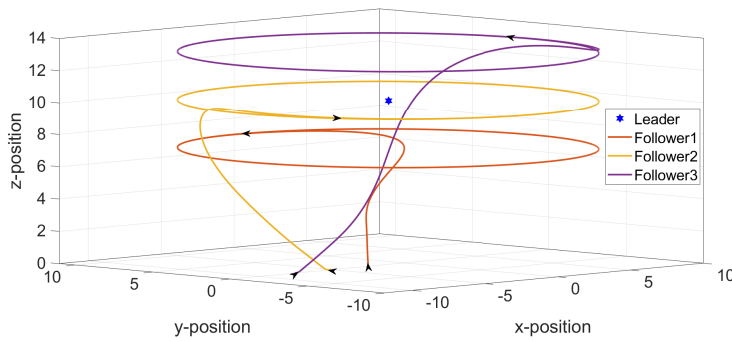


Fig. 5: Formation tracking with a hovering leader

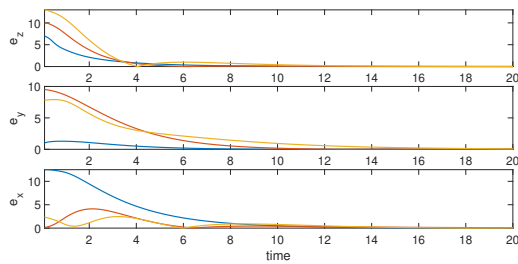


Fig. 6: Tracking error with a stationary leader

372 In the second scenario, the leader is moving with  $\mu_{x0} = 0.03\text{m/s}^2$ ,  $\mu_{y0} =$   
 373  $-0.01\text{m/s}^2$ , and  $\mu_{z0} = 0.03\cos(2\pi t/200)\text{m/s}^2$ . Figure 7 depicts the formation  
 374 tracking result. Since the leader is moving with some acceleration, only practical  
 375 formation tracking is achieved as discussed in Remark 4 and it is evident  
 376 from the tracking error shown in Figure 8. An example of sampling periods at  
 377 which the translation position is shared among the quadrotors is illustrated in  
 Figure 9.

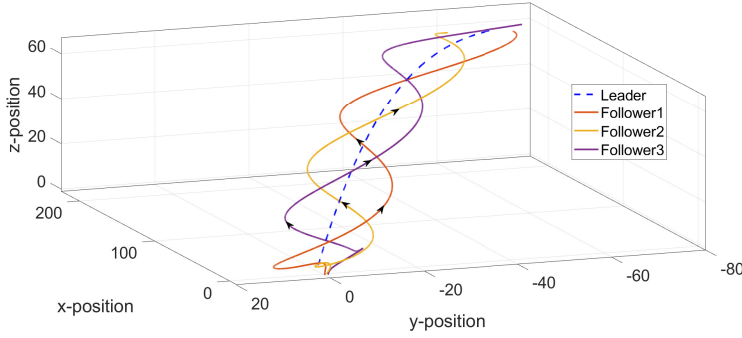


Fig. 7: Formation tracking with a moving leader

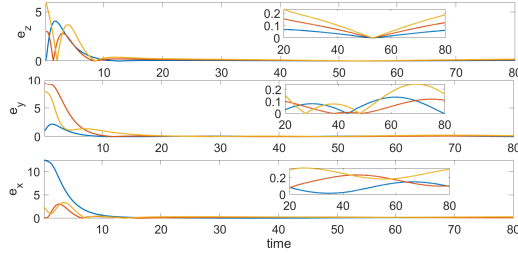


Fig. 8: Tracking error with a moving leader

378

## 379 6 Conclusion

380 In this paper, a time-varying formation tracking controller for multi-quadrotor  
 381 systems is discussed. The quadrotors can only send their translation position  
 382 information to their neighbors at asynchronous and nonuniform sampling rate.  
 383 The overall control of quadrotor is divided into a position and an attitude control  
 384 loops. An observer-based position controller is used to achieve the desired  
 385 formation, while a finite-time controller is used to control the Euler angles

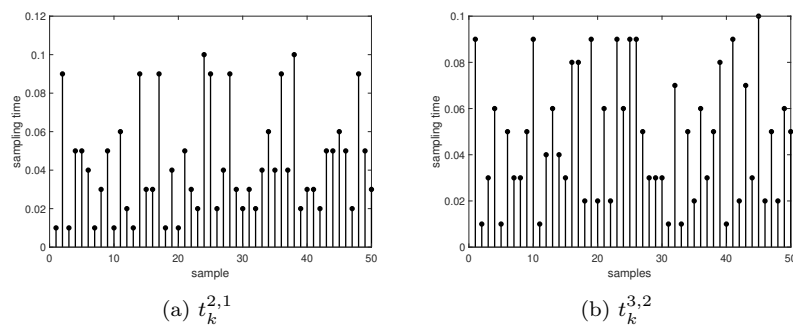


Fig. 9: Sampling periods

386 of the quadrotor such that it follows the required translation trajectory. A  
 387 closed-loop stability analysis which includes both position and attitude con-  
 388 trollers and the nonlinear coupling strength is provided. Simulation results  
 389 show the efficiency of the proposed algorithm. The case of switching topology  
 390 with adaptive gains is planned in the future.

## 391 7 Declaration

### 392 7.1 Funding

393 This work was financially supported by European Commission through ECSEL-  
 394 JU 2018 program under grant agreement No. 826610. The third author was  
 395 partially supported by the Hauts-de-France region under project ANR I2RM.

### 396 7.2 Conflicts of interest

397 Authors declare that they have no conflict of interest.

### 398 7.3 Code availability

399 Not applicable.

### 400 7.4 Authors' Contributions

### 401 7.5 Availability of data and material

402 Not applicable.

403 7.6 Ethics approval

404 Not applicable.

405 7.7 Consent to participate

406 Not applicable.

407 7.8 Consent for publication

408 Not applicable.

#### 409 **Appendix A**

410 *Proof* Let  $v = \min\left(\frac{a}{\sqrt{2}}, \frac{b}{\sqrt{2}}\right)$ ,  $\xi = 2\frac{c\delta}{b}$  and  $\kappa = 1 - \xi$ . Since  $\delta \in (0, \varrho \min(\frac{b}{c}, \frac{1}{\sigma}))$ ,  
411 one has

$$0 < 2\frac{c\delta}{b} < 2\frac{c}{b}\varrho \min\left(\frac{b}{c}, \frac{1}{\sigma}\right) \leq 2\varrho \Rightarrow 1 - 2\varrho < \underbrace{1 - \xi}_{=\kappa} < 1 \quad (46)$$

$$0 < v\kappa\delta < v\delta < v\varrho \min\left(\frac{b}{c}, \frac{1}{\sigma}\right) \leq \sqrt{2}\varrho \quad (47)$$

412 Then  $\varrho > 0$  can be chosen, independently of  $a, b, c, k$  such that for all  $\delta \in$   
413  $(0, \varrho \min(\frac{b}{c}, \frac{1}{\sigma}))$  we have

$$\kappa \in \left(\frac{1}{\sqrt{2}}, 1\right) \quad (48)$$

$$e^{v\kappa\delta} \leq 1 + 2v\kappa\delta \quad (49)$$

414 Consider the following Lyapunov function

$$W(v_t) = v_1^2(t) + v_2^2(t) + c \int_0^\delta \int_{t-s}^t e^{v\kappa(\mu-t+s)} v_2^2(\mu) d\mu ds \quad (50)$$

415 where  $v_t(s) = [v_1(t+s), v_2(t+s)]^T$ ,  $s \in [-\delta, 0]$ . One has

$$\dot{W}(v_t) = \frac{d}{dt} (v_1^2(t) + v_2^2(t)) + c \int_0^\delta \frac{d}{dt} \int_{t-s}^t e^{v\kappa(\mu-t+s)} v_2^2(\mu) d\mu ds.$$

416 Applying Leibniz integration leads to

$$\begin{aligned}
\dot{W}(v_t) &= -av_1^2(t) - bv_2^2(t) + g(t)(v_1^2(t) + v_2^2(t)) - v\kappa c \int_0^\delta \int_{t-s}^t e^{v\kappa(\mu-t+s)} v_2^2(\mu) d\mu ds \\
&\quad + c \int_0^\delta e^{v\kappa s} v_2^2(t) - v_2^2(t-s) ds \\
&\leq -av_1^2(t) - bv_2^2(t) + c \int_{t-\delta}^t v_2^2(s) ds + g(t)(v_1^2(t) + v_2^2(t)) + k \\
&\quad - v\kappa c \int_0^\delta \int_{t-s}^t e^{v\kappa(\mu-t+s)} v_2^2(\mu) d\mu ds + c \int_0^\delta e^{v\kappa s} v_2^2(t) ds - c \int_0^\delta v_2^2(t-s) ds \\
&\leq -av_1^2(t) - bv_2^2(t) + g(t)W(v_t) + k + c \left( \frac{e^{v\kappa\delta} - 1}{v\kappa} \right) v_2^2(t) \\
&\quad - v\kappa (W(v_t) - v_1^2(t) - v_2^2(t))
\end{aligned}$$

417 Since  $\frac{e^{v\kappa\delta} - 1}{v\kappa} \leq 2\delta$  and given the definition of  $v$ , the following inequalities are  
418 achieved

$$\begin{aligned}
\dot{W}(v_t) + (v\kappa - g(t)) W(v_t) &\leq (-a + v\kappa) v_1^2(t) + (-b + 2c\delta + v\kappa) v_2^2(t) + k \\
\dot{W}(v_t) + (v\kappa - g(t)) W(v_t) &\leq -a \left( 1 - \frac{1}{\sqrt{2}} \right) v_1^2(t) - b \left( 1 - (1 - \kappa) - \frac{\kappa}{\sqrt{2}} \right) v_2^2(t) + k \\
\dot{W}(v_t) + (v\kappa - g(t)) W(v_t) &\leq -a \left( \frac{\sqrt{2} - 1}{\sqrt{2}} \right) v_1^2(t) - b\kappa \left( \frac{\sqrt{2} - 1}{\sqrt{2}} \right) v_2^2(t) + k \\
\dot{W}(v_t) &\leq (-v\kappa + g(t)) W(v_t) + k
\end{aligned}$$

419 since  $v\kappa \geq \sigma$ , so

$$\dot{W}(v_t) \leq (-\sigma + g(t)) W(v_t) + k$$

420 To get over-estimation of  $W(t)$ , let us consider the following differential equa-  
421 tion

$$\dot{W}(v_t) + (\sigma - g(t)) W(v_t) = k$$

422 The solution of the above differential equation can be given as

$$\begin{aligned}
W(v_t) &= e^{\int_0^t -\sigma + g(\mu) d\mu} W(0) + e^{\int_0^t \sigma + g(\mu) d\mu} \int_0^t e^{\int_0^s \sigma - g(\mu) d\mu} k ds \\
&= e^{\int_0^t -\sigma + g(\mu) d\mu} W(0) + \int_0^t e^{\int_s^t -\sigma + g(\mu) d\mu} k ds
\end{aligned} \tag{51}$$

423 Furthermore, one has

$$\int_0^t e^{\int_s^t -\sigma + g(\mu) d\mu} k ds = \int_0^t e^{-\sigma(t-s)} e^{\int_s^t g(\mu) d\mu} k ds$$

and since  $g(t) = 0$  for  $t > t^*$ ,

$$\begin{aligned} \int_0^t e^{\int_s^t -\sigma + g(\mu) d\mu} k ds &= \int_0^{t^*} e^{-\sigma(t-s)} e^{\int_s^{t^*} g(\mu) d\mu} k ds + \int_{t^*}^t e^{-\sigma(t-s)} k ds \\ &\leq \bar{\gamma} \int_0^{t^*} e^{-\sigma(t-s)} k ds + \int_{t^*}^t e^{-\sigma(t-s)} k ds \end{aligned}$$

424 where  $\bar{\gamma} = e^{\int_0^{t^*} g(\mu) d\mu}$ . Hence, we have

$$\begin{aligned} \int_0^t e^{\int_s^t -\sigma + g(\mu) d\mu} k ds &\leq \bar{\gamma} e^{-\sigma t} \left[ \frac{e^{\sigma t^*}}{\sigma} k - \frac{k}{\sigma} \right] + e^{-\sigma t} \left[ \frac{e^{\sigma t}}{\sigma} k - \frac{e^{\sigma t^*}}{\sigma} k \right] \\ &\leq \frac{\bar{\gamma} k}{\sigma} \left[ e^{\sigma(t^*-t)} - e^{-\sigma t} \right] + \frac{k}{\sigma} \left[ 1 - e^{\sigma(t^*-t)} \right] \end{aligned} \quad (52)$$

425 Using (52), (51) becomes

$$\begin{aligned} W(v_t) &\leq \bar{\gamma} e^{-\sigma t} W(0) + \frac{\bar{\gamma} k}{\sigma} \left[ e^{\sigma(t^*-t)} - e^{-\sigma t} \right] + \frac{k}{\sigma} \left[ 1 - e^{\sigma(t^*-t)} \right] \\ &\leq \gamma e^{-\sigma t} W(0) + \frac{\bar{\gamma} k}{\sigma} \left[ 1 - e^{-\sigma t} \right] \\ &\leq \left( \bar{\gamma} W(0) - \frac{\gamma k}{\sigma} \right) e^{-\sigma t} + \frac{\gamma k}{\sigma} \end{aligned} \quad (53)$$

426 where  $\gamma = \max\{1, \bar{\gamma}\}$ . Choosing  $\bar{\alpha} = \bar{\gamma} W(0) - \frac{\gamma k}{\sigma}$  finishes the proof.

## 427 Appendix B

428 One has

$$\begin{aligned} &2K_1(e_\xi)^T [\Omega \otimes QB] F_\Delta \\ &= 2K_1(e_\xi)^T [\Omega \otimes Q] [I_N \otimes B] F_\Delta \\ &\leq 2K_1 \sqrt{(e_\xi)^T [\Omega \otimes Q] e_\xi} \sqrt{[(I_N \otimes B] F_\Delta]^T [\Omega \otimes Q] (I_N \otimes B) F_\Delta} \end{aligned}$$

429 Using the Cauchy-Schwarz inequality one obtains

$$K_1(e_\xi)^T [(\Omega \otimes (QB))] F_\Delta \leq 2K_1 \sqrt{V_c} \sqrt{\lambda_{\max}(\Omega \otimes Q)} \|I_N \otimes B\| \|F_\Delta\|$$

430 and using Rayleigh inequality one has

$$K_1(e_\xi)^T [(\Omega \otimes (QB))] F_\Delta \leq 2K_1 \sqrt{V_c} \sqrt{\omega_{\max} \lambda_{\max}(Q)} \|F_\Delta\| \quad (54)$$

431 Over estimation of term  $\|F_\Delta\|$  gives

$$\|F_\Delta\| \leq \sum_{i=1}^N \left\| \frac{T_i}{m_i} H_i \right\|$$

432 with

$$\left\| \frac{T_i}{m_i} H_i \right\| = \frac{1}{m_i} |T_i(e_{\xi_i})| \|H_i\| \quad (55)$$

$$= \frac{1}{m_i} |T_i(e_{\xi_i})| \sqrt{h_1^2 + h_2^2 + h_3^2} \quad (56)$$

433 where

$$|T_i(e_{\xi_i})| = m_i \|\mu_i + g e_3\| = m_i \sqrt{\mu_{x_i}^2 + \mu_{y_i}^2 + (\mu_{z_i} + g)^2}. \quad (57)$$

434 Following the proof of [26, Theorem 1], one has

$$\|\mu_i\| = \|\mu_i^f\| \leq c_4 \sum_{i=1}^N \|e_{\xi_i}\| + c_5 \sum_{k=0}^N s_{i,k} \|\bar{x}_{i,k}\| \quad (58)$$

435 where  $c_4, c_5 > 0$ . So, we obtain

$$\|T_i\| \leq m_i \left( g + c_6 \left\{ \sum_{i=1}^N \|e_{\xi_i}\| + \sum_{k=0}^N s_{i,k} \|\bar{x}_{i,k}\| \right\} \right) \quad (59)$$

$$\leq l_1 \left( r_1 + \sum_{i=1}^N \|e_{\xi_i}\| + \sum_{k=0}^N s_{i,k} \|\bar{x}_{i,k}\| \right) \quad (60)$$

436 where  $c_6 = \max(c_4, c_5)$ ,  $l_1 = m_i c_6$  and  $r_1 = m_i g / l_1$ . From these inequalities,  
437 one can deduce that

$$|T_i(e_{\xi_i})| \leq \begin{cases} r_2 \bar{e}_i & \text{for } \bar{e}_i \geq r_1 \\ r_1 r_2 & \text{for } \bar{e}_i < r_1 \end{cases} \quad (61)$$

438 where  $\bar{e}_i = \sum_{i=1}^N \|e_{\xi_i}\| + \sum_{k=0}^N \|\bar{x}_{i,k}\|$  and  $r_2 = 2l_1$ .

439 Now replacing  $(\phi_i, \theta_i, \psi_i)$  with  $(\phi_{di} + e_{\phi_i}, \theta_{di} + e_{\theta_i}, \psi_{di} + e_{\psi_i})$  and using the  
440 following trigonometric equalities

$$\sin(a + b) = \sin(a) + \sin\left(\frac{b}{2}\right) \cos\left(a + \frac{b}{2}\right) \quad (62)$$

$$\cos(a + b) = \cos(a) - \sin\left(\frac{b}{2}\right) \sin\left(a + \frac{b}{2}\right) \quad (63)$$

441 then  $h_3$  can be written as

$$\begin{aligned} h_3 &= c\phi_i c\theta_i - c\phi_{di} c\theta_{di} \\ &= c(\phi_{di} + e_{\phi_i})c(\theta_{di} + e_{\theta_i}) - c\phi_{di} c\theta_{di} \\ &= [c\phi_{di} - s(e_{\phi_i}/2)s(\phi_{di} + e_{\phi_i}/2)][c\theta_{di} - s(e_{\theta_i}/2)s(\theta_{di} + e_{\theta_i}/2)] - c\phi_{di} c\theta_{di} \\ &= -c\phi_{di} s(e_{\theta_i}/2)s(\theta_{di} + e_{\theta_i}/2) - c\theta_{di} s(e_{\phi_i}/2)s(\phi_{di} + e_{\phi_i}/2) \\ &\quad + [-s(e_{\phi_i}/2)s(\phi_{di} + e_{\phi_i}/2)][s(e_{\theta_i}/2)s(\theta_{di} + e_{\theta_i}/2)] \end{aligned}$$

442 Using the following trivial inequalities

$$\begin{aligned} |\sin(a)| &\leq |a|, & |\sin(a)| &\leq 1, & |\cos(a)| &\leq 1 \\ |a||b| &\leq \frac{1}{2}(|a| + |b|) \text{ for } |a| \leq 1, |b| \leq 1 \\ |a||b||c| &\leq \frac{1}{2}(|a| + |b| + |c|) \text{ for } |a| \leq 1, |b| \leq 1, |c| \leq 1 \end{aligned} \quad (64)$$

443 one gets

$$\begin{aligned} |h_3| &\leq |s(e_{\phi_i}/2)| + |s(e_{\theta_i}/2)| + |s(e_{\phi_i}/2)||s(e_{\theta_i}/2)| \\ &\leq |s(e_{\phi_i}/2)| + |s(e_{\theta_i}/2)| + \frac{1}{2}(|s(e_{\phi_i}/2)| + |s(e_{\theta_i}/2)|) \\ &\leq \frac{3}{2}(|s(e_{\phi_i}/2)| + |s(e_{\theta_i}/2)|) \\ &\leq \frac{3}{4}(|e_{\phi_i}| + |e_{\theta_i}|) \end{aligned} \quad (65)$$

444 Therefore, the following inequality can be obtained

$$\begin{aligned} h_3^2 &\leq \frac{9}{16}(e_{\phi_i}^2 + e_{\theta_i}^2 + 2|e_{\phi_i}||e_{\theta_i}|) \\ &\leq \frac{9}{8}(e_{\phi_i}^2 + e_{\theta_i}^2) \\ &\leq \varsigma_3(e_{\phi_i}^2 + e_{\theta_i}^2 + e_{\psi_i}^2) \end{aligned} \quad (66)$$

445 where  $\varsigma_3 = \frac{9}{8}$ . Similarly, one can show that

$$h_2^2 \leq \varsigma_2(e_{\phi_i}^2 + e_{\theta_i}^2 + e_{\psi_i}^2) \quad (67)$$

$$h_1^2 \leq \varsigma_1(e_{\phi_i}^2 + e_{\theta_i}^2 + e_{\psi_i}^2) \quad (68)$$

446 Therefore, one gets

$$\begin{aligned} \|H(e_{\xi_i}, e_{\eta_i})\| &= \sqrt{h_1^2 + h_2^2 + h_3^2} \\ &\leq \sqrt{\varsigma_1(e_{\phi_i}^2 + e_{\theta_i}^2 + e_{\psi_i}^2) + \varsigma_2(e_{\phi_i}^2 + e_{\theta_i}^2 + e_{\psi_i}^2) + \varsigma_3(e_{\phi_i}^2 + e_{\theta_i}^2 + e_{\psi_i}^2)} \\ &\leq c_7 \|\eta_i - \eta_{d_i}\| \end{aligned} \quad (69)$$

447 with  $c_7 = \sqrt{\varsigma_1 + \varsigma_2 + \varsigma_3}$

448 From (61) and (69), one can show that for  $\bar{e}_i \geq r_1$

$$\begin{aligned} \left\| \frac{T_i}{m_i} H_i \right\| &\leq \frac{1}{m_i} r_2 \bar{e}_i c_7 \|e_{\eta_i}\| \\ &\leq c_8 \|e_{\eta_i}\| \bar{e}_i \end{aligned}$$

449 with  $c_8 = \frac{1}{m_i} r_2 c_7$ . So one has

$$\left\| \frac{T_i}{m_i} H_i \right\| \leq c_8 \|e_{\eta_i}\| \left[ \sum_{i=1}^N \|e_{\xi_i}\| + \sum_{k=0}^N s_{i,k} \|\bar{x}_{i,k}\| \right] \quad (70)$$

450 Since

$$\sum_{i=1}^N \|e_{\xi_i}\| \leq \frac{\sqrt{N}}{\sqrt{\lambda_{\min}(Q)}\sqrt{\omega_{\min}}} \sqrt{V_c(e_{\xi}^c)}$$

451 and

$$\|\bar{x}_{i,k}\| \leq \frac{1}{\sqrt{\lambda_{\min}(P)}} \sqrt{V_o(\bar{x}_{i,k})}$$

452 inequality (70) becomes

$$\left\| \frac{T_i}{m_i} H_i \right\| \leq c_8 c_9 \|e_{\eta_i}\| \left[ \sqrt{V_c(e_{\xi}^c)} + \sum_{k=0}^N s_{i,k} \sqrt{V_o(\bar{x}_{i,k})} \right]$$

453 with  $c_9 = \max\left(\frac{\sqrt{N}}{\sqrt{\lambda_{\min}(Q)}\sqrt{\omega_{\min}}}, \frac{1}{\sqrt{\lambda_{\min}(P)}}\right)$ . On can write the above inequality

454 as

$$\left\| \frac{T_i}{m_i} H_i \right\| \leq \chi \|e_{\eta_i}\| \left[ \sqrt{V_c(e_{\xi}^c)} + \sum_{k=0}^N s_{i,k} \sqrt{V_o(\bar{x}_{i,k})} \right] \quad (71)$$

455 where  $\chi = c_8 c_9$  which leads to

$$\|F_{\Delta}\| \leq \sum_{i=1}^N \chi (\|e_{\eta_i}\|) \left[ \sqrt{V_c(e_{\xi}^c)} + \sum_{k=0}^N s_{i,k} \sqrt{V_o(\bar{x}_{i,k})} \right] \quad (72)$$

456 Hence, inequality (54) is achieved.

## 457 References

- 458 1. Zhao, Z., Cao, D., Yang, J., Wang, H.: High-order sliding mode observer-  
459 based trajectory tracking control for a quadrotor uav with uncertain dy-  
460 namics. *Nonlinear Dynamics* **102**(4), 2583–2596 (2020)
- 461 2. Shakhathreh, H., Sawalmeh, A.H., Al-Fuqaha, A., Dou, Z., Almaita, E.,  
462 Khalil, I., Othman, N.S., Khreishah, A., Guizani, M.: Unmanned aerial  
463 vehicles (uavs): A survey on civil applications and key research challenges.  
464 *Ieee Access* **7**, 48572–48634 (2019)
- 465 3. Mishra, B., Garg, D., Narang, P., Mishra, V.: Drone-surveillance for search  
466 and rescue in natural disaster. *Computer Communications* **156**, 1–10  
467 (2020)
- 468 4. Eskandarpour, A., Sharf, I.: A constrained error-based mpc for path fol-  
469 lowing of quadrotor with stability analysis. *Nonlinear Dynamics* **99**(2),  
470 899–918 (2020)
- 471 5. Iskandarani, M., Hafez, A.T., Givigi, S.N., Beaulieu, A., Rabbath, C.A.:  
472 Using multiple quadrotor aircraft and linear model predictive control for  
473 the encirclement of a target. In: 2013 IEEE International Systems Con-  
474 ference (SysCon), pp. 620–627. IEEE (2013)

- 475 6. Hou, Z., Wang, W., Zhang, G., Han, C.: A survey on the formation control of multiple quadrotors. In: 2017 14th International Conference on Ubiquitous Robots and Ambient Intelligence (URAI), pp. 219–225. IEEE (2017)
- 476
- 477
- 478
- 479 7. Sivakumar, A., Tan, C.K.Y.: Uav swarm coordination using cooperative control for establishing a wireless communications backbone. In: Proceedings of the 9th International Conference on Autonomous Agents and Multiagent Systems: Volume 3-Volume 3, pp. 1157–1164 (2010)
- 480
- 481
- 482
- 483 8. Yao, X.Y., Ding, H.F., Ge, M.F.: Fully distributed control for task-space formation tracking of nonlinear heterogeneous robotic systems. *Nonlinear Dynamics* **96**(1), 87–105 (2019)
- 484
- 485
- 486 9. Lippay, Z.S., Hoagg, J.B.: Leader-following formation control with time-varying formations and bounded controls for agents with double-integrator dynamics. In: 2020 American Control Conference (ACC), pp. 871–876. IEEE (2020)
- 487
- 488
- 489
- 490 10. Van Vu, D., Trinh, M.H., Nguyen, P.D., Ahn, H.S.: Distance-based formation control with bounded disturbances. *IEEE Control Systems Letters* **5**(2), 451–456 (2020)
- 491
- 492
- 493 11. Li, S., Zhang, J., Li, X., Wang, F., Luo, X., Guan, X.: Formation control of heterogeneous discrete-time nonlinear multi-agent systems with uncertainties. *IEEE Transactions on Industrial Electronics* **64**(6), 4730–4740 (2017)
- 494
- 495
- 496
- 497 12. Yu, J., Dong, X., Li, Q., Ren, Z.: Practical time-varying formation tracking for high-order nonlinear multi-agent systems based on the distributed extended state observer. *International Journal of Control* **92**(10), 2451–2462 (2019)
- 498
- 499
- 500
- 501 13. Qin, D., Liu, A., Zhang, D., Ni, H.: Formation control of mobile robot systems incorporating primal-dual neural network and distributed predictive approach. *Journal of the Franklin Institute* **357**(17), 12454–12472 (2020)
- 502
- 503
- 504 14. Nag, S., Summerer, L.: Behaviour based, autonomous and distributed scatter manoeuvres for satellite swarms. *Acta Astronautica* **82**(1), 95–109 (2013)
- 505
- 506
- 507 15. Mercado, D., Castro, R., Lozano, R.: Quadrotors flight formation control using a leader-follower approach. In: 2013 European Control Conference (ECC), pp. 3858–3863. IEEE (2013)
- 508
- 509
- 510 16. Ren, W.: Consensus strategies for cooperative control of vehicle formations. *IET Control Theory & Applications* **1**(2), 505–512 (2007)
- 511
- 512 17. Du, H., Li, S., Lin, X.: Finite-time formation control of multiagent systems via dynamic output feedback. *International Journal of Robust and Nonlinear Control* **23**(14), 1609–1628 (2013)
- 513
- 514
- 515 18. Dong, X., Zhou, Y., Ren, Z., Zhong, Y.: Time-varying formation tracking for second-order multi-agent systems subjected to switching topologies with application to quadrotor formation flying. *IEEE Transactions on Industrial Electronics* **64**(6), 5014–5024 (2016)
- 516
- 517
- 518
- 519 19. Xiong, T., Pu, Z., Yi, J., Tao, X.: Fixed-time observer based adaptive neural network time-varying formation tracking control for multi-agent
- 520

- 521 systems via minimal learning parameter approach. *IET Control Theory*  
522 & *Applications* **14**(9), 1147–1157 (2020)
- 523 20. Lai, J., Chen, S., Lu, X., Zhou, H.: Formation tracking for nonlinear multi-  
524 agent systems with delays and noise disturbance. *Asian Journal of Control*  
525 **17**(3), 879–891 (2015)
- 526 21. Kuriki, Y., Namerikawa, T.: Consensus-based cooperative formation control  
527 with collision avoidance for a multi-uav system. In: 2014 American  
528 Control Conference, pp. 2077–2082. IEEE (2014)
- 529 22. Wang, Y., Wu, Q., Wang, Y.: Distributed cooperative control for multiple  
530 quadrotor systems via dynamic surface control. *Nonlinear Dynamics*  
531 **75**(3), 513–527 (2014)
- 532 23. Zou, Y., Zhou, Z., Dong, X., Meng, Z.: Distributed formation control  
533 for multiple vertical takeoff and landing uavs with switching topologies.  
534 *IEEE/ASME Transactions on Mechatronics* **23**(4), 1750–1761 (2018)
- 535 24. Zhang, W., Chaoyang, D., Maopeng, R., Yang, L.: Fully distributed time-  
536 varying formation tracking control for multiple quadrotor vehicles via  
537 finite-time convergent extended state observer. *Chinese Journal of Aero-*  
538 *navics* **33**(11), 2907–2920 (2020)
- 539 25. Cong, Y., Du, H., Jin, Q., Zhu, W., Lin, X.: Formation control for multi-  
540 quadrotor aircraft: Connectivity preserving and collision avoidance. *Inter-*  
541 *national Journal of Robust and Nonlinear Control* **30**(6), 2352–2366  
542 (2020)
- 543 26. Ajwad, S.A., Menard, T., Moulay, E., Defoort, M., Coirault, P.: Observer  
544 based leader-following consensus of second-order multi-agent systems with  
545 nonuniform sampled position data. *Journal of the Franklin Institute*  
546 **356**(16), 10031–10057 (2019)
- 547 27. Ajwad, S.A., Moulay, E., Defoort, M., Ménard, T., Coirault, P.: Output-  
548 feedback formation tracking of second-order multi-agent systems with  
549 asynchronous variable sampled data. In: 2019 IEEE 58th Conference on  
550 Decision and Control (CDC), pp. 4483–4488. IEEE (2019)
- 551 28. Ajwad, S.A., Moulay, E., Defoort, M., Ménard, T., Coirault, P.: Collision-  
552 free formation tracking of multi-agent systems under communication con-  
553 straints. *IEEE Control Systems Letters* **5**(4), 1345–1350 (2020)
- 554 29. Menard, T., Ajwad, S.A., Moulay, E., Coirault, P., Defoort, M.: Leader-  
555 following consensus for multi-agent systems with nonlinear dynamics sub-  
556 ject to additive bounded disturbances and asynchronously sampled out-  
557 puts. *Automatica* **121**, 109176 (2020)
- 558 30. Kendoul, F.: Nonlinear hierarchical flight controller for unmanned rotor-  
559 craft: design, stability, and experiments. *Journal of guidance, control, and*  
560 *dynamics* **32**(6), 1954–1958 (2009)
- 561 31. Zhao, B., Xian, B., Zhang, Y., Zhang, X.: Nonlinear robust adaptive tracking  
562 control of a quadrotor uav via immersion and invariance methodology.  
563 *IEEE Transactions on Industrial Electronics* **62**(5), 2891–2902 (2014)
- 564 32. Ren, W., Beard, R.W.: *Distributed consensus in multi-vehicle cooperative*  
565 *control*, vol. 27. Springer (2008)

- 
- 566 33. Song, Q., Liu, F., Cao, J., Yu, W.: Pinning-controllability analysis of com-  
567     plex networks: an m-matrix approach. *IEEE Transactions on Circuits and*  
568     *Systems I: Regular Papers* **59**(11), 2692–2701 (2012)
- 569 34. Zhang, H., Li, Z., Qu, Z., Lewis, F.L.: On constructing lyapunov functions  
570     for multi-agent systems. *Automatica* **58**, 39–42 (2015)